

# Propagation of hexagonal patterns near onset

ARJEN DOELMAN<sup>1</sup>, BJÖRN SANDSTEDE<sup>2</sup>, ARND SCHEEL<sup>3</sup>  
and GUIDO SCHNEIDER<sup>4</sup>

<sup>1</sup> Korteweg-de Vries Institute, University of Amsterdam, Plantage Muidergracht 24,  
1018 TV Amsterdam, The Netherlands

<sup>2</sup> Department of Mathematics, The Ohio State University, 231 West 18th Avenue,  
Columbus, OH 43210, USA

<sup>3</sup> Department of Mathematics, University of Minnesota, 127 Vincent Hall,  
206 Church St. S.E., Minneapolis, MN 55455, USA

<sup>4</sup> Mathematisches Institut I, Universität Karlsruhe, 76128 Karlsruhe, Germany

(Received 24 October 2001; revised 5 March 2002)

Dedicated to Klaus Kirchgässner on the occasion of his seventieth birthday with our deep  
gratitude for his encouragement, mentorship and support.

For a pattern-forming system with two unbounded spatial directions that is near the onset to instability, we prove the existence of modulated fronts that connect (i) stable hexagons with the unstable trivial pattern, (ii) stable hexagons with unstable roll solutions, (iii) stable hexagons with unstable hexagons, and (iv) stable roll solutions with unstable hexagons. Our approach is based on spatial dynamics, bifurcation theory, and geometric singular perturbation theory.

## 1 Introduction

Over the past few decades, the spontaneous formation of patterns in spatially extended systems has attracted much attention. Many beautiful patterns such as spatially periodic rolls, hexagonal cell structures, and spiral waves have been observed in experiments [4, 11]. Among the experiments where these patterns occur are the Rayleigh–Bénard convection [1] and chemical reactions such as the chlorite-iodide-malonic acid reaction (CIMA) [2, 35]. Different patterns may compete in a spatial region, leading to the formation of interfaces that may or may not propagate. See elsewhere [4, 1, 2, 13] for details and further references.

Mathematically, the existence of spatially periodic patterns such as rolls or hexagons can be predicted from a linear stability analysis of the homogeneous background solution that corresponds to the pure conduction state in the Rayleigh–Bénard convection and to a homogeneous mixture of chemicals in the CIMA reaction. If the physical system is isotropic, homogeneous, and essentially two-dimensional, then any reasonable model will be invariant under the Euclidean symmetry group of the plane. Slightly beyond the onset to instability, each mode with a wavenumber  $k$  on an annulus  $|k| \sim k_c$  is amplified for some critical wavenumber  $k_c > 0$ . Fixing a lattice subgroup of the Euclidean symmetry group and restricting the model to those unstable modes that respect the fixed lattice gives spatially-periodic patterns that live on that lattice.

In experiments and numerical simulations, stable spatially-periodic patterns typically arise through small, localized perturbations of the underlying unstable background state. These perturbations grow in amplitude until nonlinear saturation takes over while, at the same time, invading the unstable background state. Whereas the spatially uniform growth into a pattern can be described within the context of amplitude equations for a finite number of modes, any explanation of propagation and spatial competition requires a description of the problem by a Partial Differential Equation (PDE) that incorporates spatial long-wavelength modulations of the amplitude.

Our goal in this paper is to investigate some of the interfaces between competing spatially-periodic patterns. We are interested in interfaces that can be modelled as *modulated fronts*, i.e. as waves that are time-periodic in an appropriate co-moving coordinate frame. Both speed and shape of these interfaces therefore vary periodically in time. We emphasize that propagating fronts that connect spatially-periodic patterns cannot possibly translate rigidly since the asymptotic spatially-periodic patterns become time-periodic in a co-moving frame. We focus on proving the existence of modulated fronts that connect stable with unstable patterns. Our analysis will also lead to conjectures on the average speed of these fronts and on the existence of modulated fronts that connect different stable patterns.

Instead of considering the full Rayleigh–Bénard problem or general reaction-diffusion systems, we focus on a modified Swift–Hohenberg equation,

$$\partial_t u = -(1 + \Delta)^2 u + \mu u - \beta |\nabla u|^2 - u^3, \quad (1.1)$$

as a phenomenological model for pattern-forming systems near the onset of instability. In the above equation, we take  $u(x, t) \in \mathbb{R}$ ,  $x = (x_1, x_2) \in \mathbb{R}^2$  and  $t \geq 0$ . The parameters  $\mu, \beta \in \mathbb{R}$  are both real. We write  $\nabla u = (\partial_{x_1} u, \partial_{x_2} u)$  for the gradient and  $\Delta = \partial_{x_1}^2 + \partial_{x_2}^2$  for the Laplace operator. Note that we recover the usual Swift–Hohenberg equation if we set  $\beta = 0$ . The additional term  $\beta |\nabla u|^2$ , reminiscent of the Kuramoto–Sivashinsky equation, breaks the symmetry  $u \mapsto -u$ . It is needed to obtain stable hexagonal patterns (see § 2).

For appropriate parameter values, (1.1) exhibits stripes and hexagonal patterns. The purpose of this paper is to prove the existence of modulated fronts which describe (see Figure 1 for an illustration)

- (i) stable hexagons that invade the unstable rest state at  $u = 0$ ,
- (ii) stable hexagons that invade unstable roll solutions,
- (iii) stable hexagons that invade unstable hexagons, and lastly,
- (iv) stable roll solutions that invade unstable hexagons.

Our analysis is based on spatial dynamics, bifurcation theory, and geometric singular perturbation theory. The main idea behind our approach has already been exploited [8, 16] for equations with only one unbounded space direction. The analysis there shows the existence of modulated fronts that describe stable roll solutions which invade the unstable homogeneous rest state. As in Collet & Eckmann [8] and Eckmann & Wayne [16], the main ingredient in our analysis is a center-manifold reduction for the spatial dynamics. On the center manifold, we derive amplitude equations for the travelling-wave problem. We refer to Haragus & Schneider [21] for a related analysis of the Taylor–Couette problem.

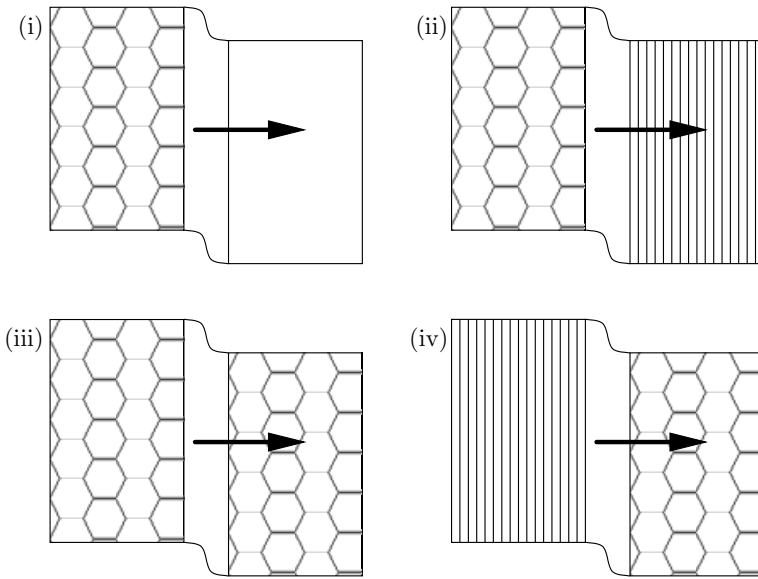


FIGURE 1. Modulated fronts connecting (i) stable hexagons to the unstable trivial pattern, (ii) stable hexagons to unstable roll solutions, (iii) stable hexagons to unstable hexagons, and (iv) stable roll solutions to unstable hexagons.

We expect that a similar reduction theorem can be proved for the Rayleigh–Bénard problem and that the resulting amplitude equations on the center manifold coincide with those derived here for the modified Swift–Hohenberg equation. In fact, as mentioned above, the modified Swift–Hohenberg equation (1.1) is a phenomenological model for Bénard’s problem. In Bénard’s problem,  $\beta = 0$  corresponds to a fixed boundary at the top, while  $\beta \neq 0$  corresponds to a free boundary at the top, thus breaking the midplane-reflection symmetry. We refer to Lin *et al.* [32] for a discussion about the validity of the Swift–Hohenberg model for the Rayleigh–Bénard problem.

## 2 Existence of rolls and hexagons

In this section, we recall the existence and stability analysis of the spatially-periodic stripe and hexagon patterns for (1.1). An extensive analysis of the general type of bifurcation that arises here can be found in Golubitsky *et al.* [19] and the literature cited therein. In particular, we do not claim any originality for the results presented in this section. As mentioned above, the approach pursued here consists of analysing the bifurcations of the homogeneous rest state restricted to the space of functions with hexagonal symmetry. On this space, we can apply classical reduction methods of bifurcation theory such as the Lyapunov–Schmidt method [7] or the center-manifold theorem [24] to find bifurcating spatially-periodic patterns. For  $\beta = 0$ , this analysis shows that the bifurcating hexagons are generically unstable [19]. Thus, stable hexagons of small amplitude can only be found for  $\beta \neq 0$ .

We begin by linearizing (1.1) about the homogeneous rest state  $u = 0$ , which gives

$$\partial_t v = -(1 + \Delta)^2 v + \mu v. \quad (2.1)$$

The linearized equation admits solutions of the form

$$v(x, t) = e^{\lambda t + ik_1 x_1 + ik_2 x_2}$$

for temporal growth rates  $\lambda$  and spatial wave numbers  $k = (k_1, k_2)$  that are related via the dispersion relation

$$\lambda = \lambda(k_1, k_2) = -(1 - k_1^2 - k_2^2)^2 + \mu.$$

In particular, the rest state  $u = 0$  is exponentially attracting for  $\mu < 0$ . For  $\mu > 0$ , all spatial Fourier modes associated with spatial wave numbers  $k = (k_1, k_2)$  in the annulus  $|k_1^2 + k_2^2 - 1| < \sqrt{\mu}$  have positive temporal growth rates  $\lambda$ .

Next, we restrict the modified Swift–Hohenberg equation to functions that have hexagonal symmetry. Restricted to this function space, the annulus of unstable eigenmodes breaks up into finitely many discrete eigenvalues. To be precise, consider locally square-integrable functions  $u \in L^2_{\text{loc}}(\mathbb{R}^2)$  of the form

$$u(x_1, x_2) = u\left(x_1, x_2 + \frac{4\pi}{\sqrt{3}}\right) = u\left(x_1 + 2\pi, x_2 + \frac{2\pi}{\sqrt{3}}\right). \quad (2.2)$$

Any such function can be represented by a convergent Fourier series

$$u(x_1, x_2) = \sum_{(\ell_1, \ell_2) \in \mathbb{Z}^2} \hat{u}_{\ell_1, \ell_2} e^{i\ell_1 x_1 + i\ell_2 (x_1 + \sqrt{3}x_2)/2}$$

with complex coefficients  $\hat{u}_{\ell_1, \ell_2} \in \mathbb{C}$ . Note that the initial-value problem associated with (1.1) is well-posed on the space

$$\begin{aligned} \mathcal{X} &= \left\{ u \in H^4_{\text{loc}}(\mathbb{R}^2, \mathbb{R}); u(x_1, x_2) = u\left(x_1, x_2 + \frac{4\pi}{\sqrt{3}}\right) = u\left(x_1 + 2\pi, x_2 + \frac{2\pi}{\sqrt{3}}\right), \right. \\ &\quad \left. \|u\|_{\mathcal{X}}^2 = \sum_{(\ell_1, \ell_2) \in \mathbb{Z}^2} |\hat{u}_{\ell_1, \ell_2}|^2 (1 + \ell_1^2 + \ell_2^2)^4 < \infty \right\}. \end{aligned}$$

In particular, for any  $u_0 \in \mathcal{X}$ , there exists a unique solution  $u = u(t) \in \mathcal{X}$  to (1.1) with  $u|_{t=0} = u_0$ . This solution depends smoothly on  $t > 0$  and on  $u_0 \in \mathcal{X}$ . Furthermore, the solution exists globally in time, i.e.  $u \in C^0([0, \infty), \mathcal{X})$  (see Mielke & Schneider [34] for the one-dimensional case).

For  $\mu = 0$ , the linearization (2.1) restricted to  $\mathcal{X}$  has  $\lambda = 0$  as an eigenvalue with geometric and algebraic multiplicity equal to six. The associated six eigenfunctions span the center subspace

$$\mathcal{X}_c = \text{span}\{e^{ix_1}, e^{i(-\frac{1}{2}x_1 + \frac{\sqrt{3}}{2}x_2)}, e^{i(-\frac{1}{2}x_1 - \frac{\sqrt{3}}{2}x_2)}, \text{c.c.}\}.$$

All other eigenvalues are strictly bounded away from the imaginary axis, and the associated eigenfunctions define the complementary stable subspace  $\mathcal{X}_h$  so that  $\mathcal{X} = \mathcal{X}_c \oplus \mathcal{X}_h$ . Center-manifold theory [24, 45] shows that there exists a six-dimensional, locally invariant

manifold for (1.1) that is tangential to the linear center eigenspace  $\mathcal{X}_c$  at  $u = 0$  for  $\mu = 0$ . This manifold can be constructed in such a fashion that it is invariant under the symmetries of the hexagonal lattice, generated by the rotation  $(x_1, x_2) \mapsto ((x_1 - \sqrt{3}x_2)/2, (\sqrt{3}x_1 + x_2)/2)$ , the reflection  $x_2 \mapsto -x_2$ , and the translations  $x \mapsto x + a$  for arbitrary  $a \in \mathbb{R}^2$ . Note that the center manifold is the graph of a smooth function  $h : \mathcal{U} \rightarrow \mathcal{X}_h$  that maps a small neighborhood  $\mathcal{U} \subset \mathcal{X}_c \times \mathbb{R}$  of  $(u, \mu) = 0$  in  $\mathcal{X}_c \times \mathbb{R}$  into  $\mathcal{X}_h$  with  $\|h(u_c, \mu)\|_{\mathcal{X}} \leq C(|\mu| + \|u_c\|_{\mathcal{X}})\|u_c\|_{\mathcal{X}}$  for a constant  $C$  that is independent of  $(u_c, \mu) \in \mathcal{U}$ .

Since all stationary patterns with hexagonal symmetry lie on the center manifold, it suffices to investigate the PDE restricted to the center manifold. To compute the reduced vector field, note that any element  $u$  on the center manifold can be written in a unique way as

$$u(x) = A_1 e^{ix_1} + A_2 e^{i(-\frac{1}{2}x_1 + \frac{\sqrt{3}}{2}x_2)} + A_3 e^{i(-\frac{1}{2}x_1 - \frac{\sqrt{3}}{2}x_2)} + \text{c.c.} + \tilde{h}(A, \bar{A}, \mu)$$

where the amplitudes  $A = (A_1, A_2, A_3) \in \mathbb{C}^3$  are complex and the function  $\tilde{h}$ , defined by

$$\tilde{h}(A_1, A_2, A_3, \bar{A}_1, \bar{A}_2, \bar{A}_3, \mu) = h(A_1 e^{ix_1} + A_2 e^{i(-\frac{1}{2}x_1 + \frac{\sqrt{3}}{2}x_2)} + A_3 e^{i(-\frac{1}{2}x_1 - \frac{\sqrt{3}}{2}x_2)} + \text{c.c.}, \mu),$$

satisfies the estimate

$$\|\tilde{h}(A, \bar{A}, \mu)\|_{\mathcal{X}} \leq C(|\mu| + |A| + |\bar{A}|)(|A| + |\bar{A}|).$$

Recall that stable hexagons of small amplitude can be found only for  $\beta \neq 0$ . To make the task of computing the reduced vector field on the center manifold easier, we assume that  $\beta$  is small. The flow on the center manifold can now be found by evaluating the PDE on elements of the center manifold and projecting the resulting expression orthogonally back onto the center eigenspace. Proceeding in this fashion, we obtain the reduced system

$$\begin{aligned} \partial_t A_1 &= \mu A_1 + \alpha_1 \bar{A}_2 \bar{A}_3 + \alpha_2 A_1 |A_1|^2 + \alpha_3 A_1 (|A_2|^2 + |A_3|^2) + r_1(A_1, A_2, A_3) \\ \partial_t A_2 &= \mu A_2 + \alpha_1 \bar{A}_3 \bar{A}_1 + \alpha_2 A_2 |A_2|^2 + \alpha_3 A_2 (|A_3|^2 + |A_1|^2) + r_2(A_1, A_2, A_3) \\ \partial_t A_3 &= \mu A_3 + \alpha_1 \bar{A}_1 \bar{A}_2 + \alpha_2 A_3 |A_3|^2 + \alpha_3 A_3 (|A_1|^2 + |A_2|^2) + r_3(A_1, A_2, A_3) \end{aligned} \quad (2.3)$$

(plus the complex-conjugate equations) of six Ordinary Differential Equations (ODEs) for the amplitudes that describe the flow on the center manifold. The coefficients in the above equation are real and given by

$$\alpha_1 = -\beta + O(|\beta| \mu), \quad \alpha_2 = -3 + O(|\mu| + |\beta|), \quad \alpha_3 = -6 + O(|\mu| + |\beta|). \quad (2.4)$$

These coefficients have already been computed earlier [20, (A9)] via a multi-scale expansion. The remainder terms are of higher order:  $|r_j(A)| \leq C|A|^4$ . Note that the Euclidean symmetry of the original system (1.1) with respect to rotations, reflections, and translations manifests itself in the equivariance of the reduced system with respect to

$$\begin{aligned} \sigma : (A_1, A_2, A_3) &\mapsto (\bar{A}_2, \bar{A}_3, \bar{A}_1), & \kappa : (A_1, A_2, A_3) &\mapsto (A_1, A_3, A_2), \\ \tau_a : (A_1, A_2, A_3) &\mapsto (e^{ia_1} A_1, e^{i(-a_1 + \sqrt{3}a_2)/2} A_2, e^{i(-a_1 - \sqrt{3}a_2)/2} A_3), \end{aligned}$$

respectively. The remainder terms  $r_j$  also respect these symmetries. Note that, if all

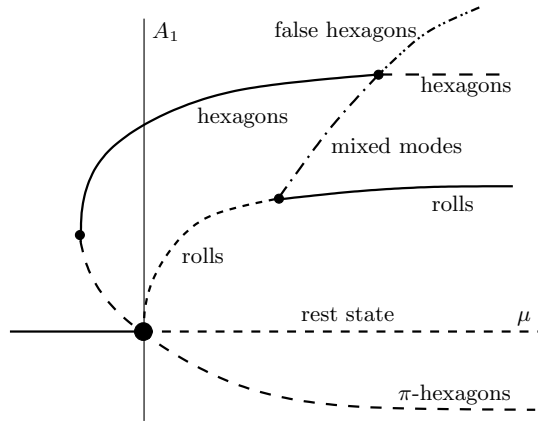


FIGURE 2. The bifurcation diagram for the modified Swift–Hohenberg equation for  $\beta < 0$  fixed and close to zero. Solid lines correspond to stable patterns, while broken lines correspond to unstable ones. The saddle-node bifurcation of hexagons occurs for  $\mu_{\text{sn}} = -\beta^2/60$ , the pitchfork bifurcation of mixed-mode solutions from rolls at  $\mu_{\text{pf}} = \beta^2/3$ , and the transcritical bifurcation of mixed-modes/false hexagons and hexagons at  $\mu_{\text{tc}} = 4\beta^2/3$ .

terms on the right-hand side of (2.3) are equally important, then  $A$  and  $\beta$  should scale with  $\sqrt{\mu}$ . This is indeed the scaling that we exploit later in (3.7). We remark that  $\sigma^2: (A_1, A_2, A_3) \mapsto (A_3, A_1, A_2)$  and  $\sigma^3: A \mapsto \bar{A}$ .

We do not attempt to give a complete description of the dynamics of (2.3), but focus instead on the existence and stability of roll solutions and hexagonal patterns. Both patterns are stationary and therefore equilibria of (2.3). Roll patterns lie in the invariant subspace  $A_1$  real and  $A_2 = A_3 = 0$ , i.e. in the intersection of the fixed-point spaces of  $\sigma^3$  and  $\tau_{(0,a_2)}$ , and correspond therefore to non-trivial stationary solutions of the ODE

$$\partial_t A_1 = \mu A_1 + \alpha_2 A_1^3 + O(|A_1|^4)$$

which exist precisely for  $\mu = (3 + O(|\beta| + |A_1|))A_1^2$ . Hexagonal patterns lie in the invariant subspace  $A_1 = A_2 = A_3$  real, i.e. in the intersection of the fixed-point spaces of  $\sigma^2$  and  $\sigma^3$ , and can therefore be found as equilibria of the ODE

$$\partial_t A_1 = \mu A_1 + \alpha_1 A_1^2 + (\alpha_2 + 2\alpha_3)A_1^3 + O(|A_1|^4).$$

Using (2.4), we see that hexagons exist for

$$\mu = \beta A_1 + (15 + O(|\beta| + |A_1|))A_1^2. \quad (2.5)$$

To determine the stability properties of rolls and hexagons with respect to perturbations that have hexagonal symmetry, it suffices to consider the linearization of (2.3) about the rolls and hexagons. We omit the relevant calculations and refer instead to Figure 2 for the complete bifurcation diagram and to §4.1 and Buzano & Golubitsky [5] and Golubitsky *et al.* [19] for further details.

### 3 Modulated front solutions

#### 3.1 Spatial dynamics

We are particularly interested in stable hexagons that invade a region occupied by either rolls or the unstable homogeneous rest state. We seek interfaces  $u(x_1, x_2, t)$  that are modulated fronts and therefore make the ansatz

$$u(x_1, x_2, t) = v(x_1 - ct, x_1, x_2), \quad (3.1)$$

where the function  $v$  shares the periodicity properties of the hexagons in its last two variables, i.e.

$$v(\xi, p_1, p_2) = v\left(\xi, p_1, p_2 + \frac{4\pi}{\sqrt{3}}\right) = v\left(\xi, p_1 + 2\pi, p_2 + \frac{2\pi}{\sqrt{3}}\right) \quad \forall (\xi, p_1, p_2). \quad (3.2)$$

Note that  $v$  also depends upon the travelling-wave variable  $\xi \in \mathbb{R}$ . In this formulation, modulated fronts that connect hexagons  $u_{\text{hex}}$  to rolls  $u_{\text{rolls}}$  or to the trivial state  $u = 0$  are given by functions  $v$  that satisfy

$$\lim_{\xi \rightarrow -\infty} v(\xi, p_1, p_2) = u_{\text{hex}}(p_1, p_2), \quad \lim_{\xi \rightarrow \infty} v(\xi, p_1, p_2) = u_{\text{right}}(p_1, p_2)$$

uniformly in the periodic variables  $(p_1, p_2)$ , where  $u_{\text{right}}$  is given by either  $u = u_{\text{rolls}}$  or  $u = 0$ .

To find modulated fronts, we substitute the ansatz (3.1) into (1.1), and obtain the equation

$$-c\partial_\xi v = -[1 + (\partial_\xi + \partial_{p_1})^2 + \partial_{p_2}^2]^2 v + \mu v - \beta[((\partial_\xi + \partial_{p_1})v)^2 + (\partial_{p_2}v)^2] - v^3. \quad (3.3)$$

In contrast to the usual travelling-wave ODE that describes rigidly-translating fronts, equation (3.3) for modulated fronts is a pseudo-elliptic PDE.

It was Kirchgässner's [29] idea to write equations of the type (3.3) as first-order differential equations in a certain function space with  $\xi$  being the new time-like variable. Even though the resulting dynamical system in  $\xi$  is typically ill-posed, it is nevertheless often possible to reduce the resulting infinite-dimensional system to a finite-dimensional one, which can then be analysed using bifurcation theory. For instance, if the linearization about the trivial rest state has only finitely many neutral eigenvalues on the imaginary axis, then (3.3) can be reduced, via center-manifold theory, to an ODE. Just as in the case of rigidly-propagating fronts, we can then find modulated fronts as heteroclinic orbits, for the spatial dynamics on the center manifold, that connect two different equilibria representing hexagons and either rolls or the background state.

The approach outlined above is often referred to as *spatial dynamics*. Since the original work of Kirchgässner, the idea of ill-posed spatial dynamics has been exploited in numerous problems. It has been adapted [16] to study small-amplitude modulated fronts in one spatial dimension, and has been further generalized [21] to the Taylor–Couette problem. Spatial dynamics has also been utilized [37, 38] to investigate bifurcations of modulated fronts with large amplitude.

Thus, we shall write (3.3) as a first-order system in the spatial variable  $\xi$ . We set

$$\mathcal{V} = (\mathcal{V}_1, \mathcal{V}_2, \mathcal{V}_3, \mathcal{V}_4) = (v, (\partial_\xi + \partial_{p_1})v, (\partial_\xi + \partial_{p_1})^2v, (\partial_\xi + \partial_{p_1})^3v), \quad (3.4)$$

and see that (3.3) is equivalent to the system

$$\begin{aligned} \partial_\xi \mathcal{V}_1 &= -\partial_{p_1} \mathcal{V}_1 + \mathcal{V}_2, \\ \partial_\xi \mathcal{V}_2 &= -\partial_{p_1} \mathcal{V}_2 + \mathcal{V}_3, \\ \partial_\xi \mathcal{V}_3 &= -\partial_{p_1} \mathcal{V}_3 + \mathcal{V}_4, \\ \partial_\xi \mathcal{V}_4 &= -\partial_{p_1} \mathcal{V}_4 + c(-\partial_{p_1} \mathcal{V}_1 + \mathcal{V}_2) + (-1 + \mu - 2\partial_{p_2}^2 - \partial_{p_2}^4) \mathcal{V}_1 - 2(1 + \partial_{p_2}^2) \mathcal{V}_3 \\ &\quad - \beta(\mathcal{V}_2^2 + (\partial_{p_2} \mathcal{V}_1)^2) - \mathcal{V}_1^3. \end{aligned} \quad (3.5)$$

Here,  $\mathcal{V}(\xi, p_1, p_2)$  lies, for each fixed  $\xi$ , in the phase-space of functions that depend on the variables  $(p_1, p_2)$  and satisfy the periodicity property (2.2) in  $(p_1, p_2)$ . In abstract form, the above equation can be written as

$$\partial_\xi \mathcal{V} = \mathcal{M}\mathcal{V} + \mathcal{N}(\mathcal{V}),$$

where the operator  $\mathcal{M} = \mathcal{M}(\partial_{p_1}, \partial_{p_2})$  represents the linear part of the equation, and the nonlinear function  $\mathcal{N}$  is given by

$$\mathcal{N}(\mathcal{V}) = (0, 0, 0, -\beta(\mathcal{V}_2^2 + (\partial_{p_2} \mathcal{V}_1)^2) - \mathcal{V}_1^3).$$

We then see that the unbounded operator

$$\mathcal{M} : H^3 \times H^2 \times H^1 \times L^2 \mapsto H^3 \times H^2 \times H^1 \times L^2$$

is closed with domain  $D(\mathcal{M}) = H^4 \times H^3 \times H^2 \times H^1$ , where each of the above Sobolev spaces consists of functions in  $(p_1, p_2)$  that satisfy

$$v(p_1, p_2) = v(p_1, p_2 + 4\pi/\sqrt{3}) = v(p_1 + 2\pi, p_2 + 2\pi/\sqrt{3}).$$

The nonlinearity  $\mathcal{N}$  is smooth when considered on the above spaces. To analyse the linear part  $\partial_\xi \mathcal{V} = \mathcal{M}\mathcal{V}$ , we use the Fourier decomposition

$$\mathcal{V}(p_1, p_2) = \sum_{(\ell_1, \ell_2) \in \mathbb{Z}^2} \mathcal{V}_{\ell_1, \ell_2} e^{i\ell_1 p_1 + i\ell_2(p_1 + \sqrt{3}p_2)/2}.$$

In the  $\mathcal{V}_{\ell_1, \ell_2}$  coordinates, the operator  $\mathcal{M}$  takes block-diagonal form with  $4 \times 4$ -matrix blocks  $\mathcal{M}_{\ell_1, \ell_2}$  on the diagonal. The matrices  $\mathcal{M}_{\ell_1, \ell_2}$  are given by

$$\mathcal{M}_{\ell_1, \ell_2} = \begin{pmatrix} -i(\ell_1 + \frac{\ell_2}{2}) & 1 & 0 & 0 \\ 0 & -i(\ell_1 + \frac{\ell_2}{2}) & 1 & 0 \\ 0 & 0 & -i(\ell_1 + \frac{\ell_2}{2}) & 1 \\ -ic(\ell_1 + \frac{\ell_2}{2}) - 1 + \mu + \frac{3\ell_2^2}{2} - \frac{9\ell_2^4}{16} & c & -2 + \frac{3\ell_2^2}{2} & -i(\ell_1 + \frac{\ell_2}{2}) \end{pmatrix}, \quad (3.6)$$

and the eigenvalue problem for each of these blocks is

$$(\mathcal{M}_{\ell_1, \ell_2} - v)\mathcal{V}_{\ell_1, \ell_2} = 0,$$

where we denote the spatial eigenvalues by  $v$ .

### 3.2 Spectra and parameter scalings

As mentioned above, we want to apply center-manifold theory to reduce (3.5) to a finite-dimensional system. Thus, we begin by discussing the spectrum of  $\mathcal{M}$  for  $\mu$  close to the threshold  $\mu = 0$ . Depending on the magnitude of the wave speed  $c$ , the spectrum of  $\mathcal{M}$  decomposes differently.

If  $c$  is bounded away from zero, there are six center eigenvalues, counted with multiplicity, and the rest of the spectrum is bounded away from the imaginary axis uniformly in  $c \geq c_0$ . In addition, the spectral projections onto the center subspace exist and are uniformly bounded for  $c \geq c_0$  (see, for instance, Ioos & Mielke [26]). Hence, in this regime, we can apply the center-manifold theorem as stated in Vanderbauwhede & Iooss [45] and arrive at a reduced six-dimensional ODE that captures all small modulated fronts. The analysis that leads to the reduced ODE in this regime is very similar to the analysis of the more complicated singular case that we shall describe below. We therefore omit the reduction analysis for the case  $c \geq c_0$  and refer instead to the subsequent analysis.

The remaining second regime occurs when the wave speed  $c$  converges to zero with the parameter  $\mu$ . In fact, this regime is the more important one since interfaces often select a modulated front that propagates with a wave speed that scales with  $\sqrt{\mu}$ . Indeed, we can find the preferred wave speed heuristically by analysing the linear dispersion relation associated with the background state  $u = 0$  in a frame that moves with speed  $c$  relative to the laboratory frame [46]. This dispersion relation is given by

$$\lambda(k; \mu, c) = -(1 - k^2)^2 + \mu + ikc.$$

Note that  $k = \pm 1$  is a double root of the dispersion relation  $\lambda(k; 0, 0)$ , i.e. we have  $\lambda(\pm 1; 0, 0) = \frac{d\lambda}{dk}(\pm 1; 0, 0) = 0$ . This double root persists for  $(\mu, c) \neq 0$  and is, to leading order, given by  $k_{db}(\mu, c) = \pm 1 + ic/8$ . The background state is convectively unstable<sup>1</sup>, i.e. solutions of the linearized equation with spatially localized initial conditions decay pointwise, precisely when  $\lambda(k_{db}; \mu, c)$  lies in the left half-plane. To leading order, we have  $\text{Re } \lambda(k_{db}; \mu, c) = \mu - c^2/16$ , so that the background state is convectively unstable for  $c > 4\sqrt{\mu}$ . The threshold value  $c_* = 4\sqrt{\mu}$  is the speed of propagation for solutions of the linear equation with spatially localized initial conditions. This critical wave speed scales with  $\sqrt{\mu}$ . We emphasize the formal nature of the above linear marginal stability criterion which is rigorous only for the linear equation and, as we shall point out in §6, probably fails in a number of interesting nonlinear cases [46, 11, 15, 47]. Thus, to capture the

<sup>1</sup> Convective instability refers to the situation where the pattern is unstable in the translation-invariant norm, but perturbations decay pointwise at any fixed point  $x$  as  $t \rightarrow \infty$ : perturbations are therefore transported towards  $|x| = \infty$ . Thus, convective instability is actually a weak type of stability.

interesting range  $c \sim \sqrt{\mu}$ , we scale the parameters  $\mu$ ,  $c$  and  $\beta$  according to

$$\mu = \varepsilon^2 \tilde{\mu}, \quad c = \varepsilon \tilde{c}, \quad \beta = \varepsilon \tilde{\beta}, \quad (3.7)$$

where  $\varepsilon$  is small and the new parameters  $\tilde{\mu}$ ,  $\tilde{c}$ , and  $\tilde{\beta}$  are  $O(1)$  in  $\varepsilon$ . The scaling of  $\beta$  with  $\sqrt{\mu}$  is motivated by the analysis of §2. Within the scaling (3.7), we expect to find all interesting modulated-front solutions.

### 3.3 Spectral gaps

Unfortunately, a major technical difficulty arises in the limit  $\varepsilon = 0$ . Each of the matrices  $\mathcal{M}_{\ell_1,1}$  generates center eigenvalues for  $(\mu, c) = 0$ , thus yielding an infinite-dimensional center eigenspace. All these eigenvalues leave the imaginary axis for  $\varepsilon > 0$ . The key to resolving this difficulty is that the center eigenvalues leave the imaginary axis with different speed. In fact, for fixed  $\tilde{c} \neq 0$ , it turns out that there are twelve center eigenvalues which stay within an  $O(\varepsilon)$ -distance of the imaginary axis, while the real parts of all other center eigenvalues scale uniformly with  $\sqrt{\varepsilon}$ . The spectral gap between these two spectral sets is of the order  $\tilde{c}\sqrt{\varepsilon}$ . In particular, for  $\varepsilon > 0$ , the infinite-dimensional center eigenspace splits into two subspaces, a twelve-dimensional subspace  $E^c$  associated with eigenvalues of distance less than  $O(\varepsilon)$  to the imaginary axis and a complement associated with eigenvalues with distance larger than  $O(\sqrt{\varepsilon})$  from the imaginary axis. The projections  $P^c$  associated with this spectral splitting are bounded uniformly in  $\varepsilon$ .

**Proposition 3.1** *For each fixed  $\tilde{c} \neq 0$  and  $\tilde{\beta}, \tilde{\mu} \in \mathbb{R}$ , there are positive constants  $d_1$ ,  $d_2$  and  $\varepsilon_0$  such that the following is true for any  $0 < \varepsilon \leq \varepsilon_0$ : the matrix  $\mathcal{M}$  has precisely twelve eigenvalues, counted with multiplicity, in the strip  $|\operatorname{Re} \lambda| \leq d_1 \varepsilon$ , while the remaining eigenvalues  $\lambda$  satisfy  $|\operatorname{Re} \lambda| \geq d_2 \sqrt{\varepsilon}$ . Furthermore, the spectral projection  $P^c$  onto the  $\varepsilon$ -dependent, twelve-dimensional eigenspace  $E^c$  associated with the eigenvalues within distance  $O(\varepsilon)$  of the imaginary axis is bounded uniformly in  $\varepsilon$ .*

The above claims can be proved as follows. Using the transformation (3.4), we see that finding eigenvalues  $v$  of the operator  $\mathcal{M}$  is equivalent to finding values of  $v$  for which the equation

$$-cvv = -[1 + (v + \partial_{p_1})^2 + \partial_{p_2}^2]^2 v + \mu v$$

has a non-trivial solution  $v$  that satisfies the periodicity condition (3.2). In Fourier space, the above equation is

$$-cv\hat{v} = -\left[1 + \left(v + i\ell_1 + \frac{i\ell_2}{2}\right)^2 - \frac{3\ell_2^2}{4}\right]^2 \hat{v} + \mu\hat{v} \quad (3.8)$$

where  $(\ell_1, \ell_2) \in \mathbb{Z}^2$ , and  $\hat{v}$  is the Fourier coefficient of  $v$  for the frequencies  $(\ell_1, \ell_2)$ . Equation (3.8) has a non-zero solution  $\hat{v}$  if, and only if,

$$-\tilde{c}\varepsilon v = -\left[1 + \left(v + i\ell_1 + \frac{i\ell_2}{2}\right)^2 - \frac{3\ell_2^2}{4}\right]^2 + \tilde{\mu}\varepsilon^2, \quad (3.9)$$

where we also used the scaling (3.7). For  $\varepsilon = 0$ , equation (3.9) reduces to

$$0 = \left[ 1 + \left( v + i\ell_1 + \frac{i\ell_2}{2} \right)^2 - \frac{3\ell_2^2}{4} \right]^2 \quad (3.10)$$

which has a solution  $v \in i\mathbb{R}$  if, and only if, either  $\ell_2 = 0$  and  $v = -i\ell_1 \pm i$  for some  $\ell_1 \in \mathbb{Z}$  or else  $\ell_2 = \pm 1$  and  $v = \pm \frac{i}{2} - i\ell_1 - \frac{i\ell_2}{2}$  for some  $\ell_1 \in \mathbb{Z}$ . In particular, there are infinitely many center eigenvalues.

We shall see that the term  $-\tilde{c}\varepsilon v$  on the left-hand side of (3.9) determines the speed with which the center eigenvalues move away from the imaginary axis upon perturbing to  $\varepsilon \neq 0$ . In particular, we expect that center eigenvalues at  $v = 0$  move away from the origin with a much slower speed. To make this precise, observe that  $v = 0$  satisfies (3.10) precisely when  $(\ell_1, \ell_2) = (\pm 1, 0), (0, \pm 1), (-1, 1)$  or  $(1, -1)$ . Switching back to the formulation (3.6) that uses the matrices  $\mathcal{M}_{\ell_1, \ell_2}$ , we see that each of the six matrices  $\mathcal{M}_{\pm 1, 0}$ ,  $\mathcal{M}_{0, \pm 1}$ ,  $\mathcal{M}_{-1, 1}$  and  $\mathcal{M}_{1, -1}$  actually has a  $2 \times 2$  Jordan block at  $v = 0$  for  $\varepsilon = 0$ . A Taylor expansion of (3.9) near  $v = 0$  for the above values of  $(\ell_1, \ell_2)$  is therefore of the form  $av^2 + \tilde{c}\varepsilon v + \tilde{\mu}\varepsilon^2 = 0$  for some non-zero number  $a \in \mathbb{C}$ . Thus, the associated twelve eigenvalues stay within a distance  $O(\varepsilon)$  of the origin in the complex plane. Next, consider the other solutions  $v$  of (3.10) that have  $\operatorname{Re} v = 0$  and  $\operatorname{Im} v \neq 0$ . If we assume that  $\tilde{c} \neq 0$ , then the term  $\tilde{c}\varepsilon v$  in (3.9) scales with  $\varepsilon$  since  $v \neq 0$  for these eigenvalues. Using standard perturbation theory, it is then not difficult to see that the correction  $\hat{v}$  defined by  $v = v|_{\varepsilon=0} + \hat{v}$  scales like  $a\sqrt{\varepsilon}$  for some  $a \neq 0$ . This completes the proof of the above claims.

Finally, we briefly comment again on the case where  $c \neq 0$ . In this case, it is easy to see that  $v = 0$  is the only purely imaginary solution of (3.8) for  $c \neq 0$  and  $\mu = 0$ . This occurs for the same values of  $(\ell_1, \ell_2)$  that were mentioned in the previous paragraph, and  $v = 0$  is in fact a simple zero of (3.8) due to the term  $-cv$ . Thus, there are only six eigenvalues on the imaginary axis. A scaling argument, which we omit, also shows that the other solutions of (3.8) for  $c \neq 0$  and  $\mu = 0$  are bounded away from the imaginary axis.

### 3.4 Existence of a center manifold

We have obtained a spectral splitting into two sets of eigenvalues that move off the imaginary axis with different speed, maintaining a spectral gap of order  $\sqrt{\varepsilon}$ . We wish to exploit this gap to find a reduction to a twelve-dimensional center manifold tangent to the center subspace  $E^c$  of the twelve eigenvalues that stay closest to the imaginary axis. A similar situation, with four rather than twelve eigenvalues, has been studied in Eckmann & Wayne [16] and Haragus & Schneider [21]. As in these references, we can indeed construct a locally invariant, twelve-dimensional center manifold that is tangent to the center eigenspace and has a diameter no less than  $\varepsilon^{\frac{3}{4}+\gamma}$  for a small positive  $\gamma < \frac{1}{4}$ . To construct this manifold, we apply [16, Theorem A.1] and follow the proof given earlier [16, Appendix A.1]. The crucial step is to show that the product of the Lipschitz constant of the nonlinearity, restricted to a ball of radius  $\varepsilon^{\frac{3}{4}+\gamma}$  centered at the rest state  $\mathcal{V}=0$ , and the inverse of the spectral gap between the center and the hyperbolic part of the linearization of (3.5) about  $\mathcal{V}=0$  is smaller than one for  $\varepsilon > 0$ . The spectral gap of the

matrix  $\mathcal{M}$  is larger than  $K_1\sqrt{\varepsilon}$  for some constant  $K_1 > 0$ , while the Lipschitz constant of the nonlinearity, restricted to a ball of radius  $\varepsilon^{\frac{3}{4}+\gamma}$ , is bounded by  $K_2\varepsilon^{\frac{1}{2}+2\gamma}$  for some constant  $K_2 > 0$ . We refer to Eckmann & Wayne [16, Appendix A.1] for further details. Thus, the product of the Lipschitz constant with the inverse of the spectral gap is of the order  $O(\varepsilon^{2\gamma})$ , and therefore certainly less than one for small  $\varepsilon > 0$ . An application of Eckmann & Wayne [16, Theorem A.1] then guarantees the existence of a center manifold of diameter  $\varepsilon^{\frac{3}{4}+\gamma}$ . The above arguments are valid for any fixed  $\tilde{c} \neq 0$  and  $\tilde{\beta}, \tilde{\mu} \in \mathbb{R}$ . In summary, we have the following proposition.

**Proposition 3.2** *For each fixed  $\tilde{c} \neq 0$ ,  $\tilde{\beta}, \tilde{\mu} \in \mathbb{R}$  and  $0 < \gamma < \frac{1}{4}$ , there is a positive constant  $\varepsilon_0$  such that the following is true for any  $0 \leq \varepsilon \leq \varepsilon_0$ : there exists a smooth map  $h : U^c \rightarrow E^h$ , where  $U^c$  is the ball of radius  $\varepsilon^{\frac{3}{4}+\gamma}$  in  $E^c$ , centered at zero, and  $E^h$  is the null space of the spectral projection  $P^c$ , such that  $h(0) = Dh(0) = 0$  and the graph of  $h$  is the locally invariant center manifold.*

We note that the spaces  $E^c$  and  $E^h$  depend on  $\varepsilon$ . We also emphasize that the modulated fronts that we shall construct below have amplitudes of order  $O(\varepsilon)$ , just like the rolls and hexagons, and are therefore certainly contained in the center manifold.

The reduced vector field on the twelve-dimensional center manifold is given by

$$\frac{d}{d\xi} \mathcal{V}^c = \mathcal{M} \mathcal{V}^c + P^c \mathcal{N}(\mathcal{V}^c + h(\mathcal{V}^c)), \quad \mathcal{V}^c \in U^c \subset E^c \quad (3.11)$$

(see Proposition 3.2). To derive an explicit expression for the right-hand side of (3.11), we follow the strategy in Eckmann & Wayne [16] and Haragus & Schneider [21], and relate the reduced equation on the center manifold to the Ginzburg–Landau equation [23, 39] of the underlying PDE (1.1).

### 3.5 The Ginzburg–Landau equation

We begin with a brief summary of the derivation of the Ginzburg–Landau equation that describes small bifurcating patterns of the Swift–Hohenberg equation (1.1) near onset. Consider solutions  $u = u(x_1, x_2)$  of (1.1) that are periodic in  $x_2$  so that  $u(x_1, x_2) = u(x_1, x_2 + 4\pi/\sqrt{3})$ . In other words, we require periodicity only in  $x_2$  but not in  $x_1$ . The dispersion relation of the linearized equation (2.1) is then given by

$$\lambda(k_1, k_2) = -(1 - k_1^2 - k_2^2)^2 + \mu$$

where  $k_1 \in \mathbb{R}$ , but  $k_2 \in \sqrt{3}\mathbb{Z}/2$  is restricted to the one-dimensional lattice spanned by  $\sqrt{3}/2$ . As illustrated in Figure 3, each curve of eigenvalues given by  $k_1 \mapsto \lambda(k_1, k_2)$  with  $k_2 = 0, \pm\sqrt{3}/2$  has exactly two maxima. In this situation, bifurcating solutions are of the form  $u = \psi + O(\varepsilon^2)$  with

$$\psi(x, t) = \varepsilon A_1(ex_1, \varepsilon^2 t) e^{ix_1} + \varepsilon A_2(ex_1, \varepsilon^2 t) e^{i(-\frac{1}{2}x_1 + \frac{\sqrt{3}}{2}x_2)} + \varepsilon A_3(ex_1, \varepsilon^2 t) e^{i(-\frac{1}{2}x_1 - \frac{\sqrt{3}}{2}x_2)} + \text{c.c.} \quad (3.12)$$

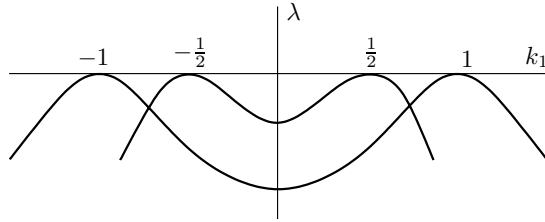


FIGURE 3. The Fourier spectrum of the linearization of (1.1) for  $\mu = 0$  with periodic boundary conditions in the  $x_2$ -direction.

where the complex amplitudes  $A_j(X, T) \in \mathbb{C}$  satisfy, to leading order, the system

$$\begin{aligned}\partial_T A_1 &= 4\partial_X^2 A_1 + \tilde{\mu}A_1 - \tilde{\beta}\overline{A}_2\overline{A}_3 - 3A_1|A_1|^2 - 6A_1(|A_2|^2 + |A_3|^2) \\ \partial_T A_2 &= \partial_X^2 A_2 + \tilde{\mu}A_2 - \tilde{\beta}\overline{A}_3\overline{A}_1 - 3A_2|A_2|^2 - 6A_2(|A_3|^2 + |A_1|^2) \\ \partial_T A_3 &= \partial_X^2 A_3 + \tilde{\mu}A_3 - \tilde{\beta}\overline{A}_1\overline{A}_2 - 3A_3|A_3|^2 - 6A_3(|A_1|^2 + |A_2|^2)\end{aligned}\quad (3.13)$$

of coupled Ginzburg–Landau equations [41]. Note that the parameters appearing in (1.1) and (3.13) are related via (3.7); see also (2.3) and (2.4). The modulated fronts that we seek correspond to front solutions  $A_j(X, T) = A_j(X - \tilde{c}T)$  of the above Ginzburg–Landau system which satisfy the ODE

$$\begin{aligned}4\partial_\zeta^2 A_1 + \tilde{c}\partial_\zeta A_1 + \tilde{\mu}A_1 - \tilde{\beta}\overline{A}_2\overline{A}_3 - 3A_1|A_1|^2 - 6A_1(|A_2|^2 + |A_3|^2) &= 0 \\ \partial_\zeta^2 A_2 + \tilde{c}\partial_\zeta A_2 + \tilde{\mu}A_2 - \tilde{\beta}\overline{A}_3\overline{A}_1 - 3A_2|A_2|^2 - 6A_2(|A_3|^2 + |A_1|^2) &= 0 \\ \partial_\zeta^2 A_3 + \tilde{c}\partial_\zeta A_3 + \tilde{\mu}A_3 - \tilde{\beta}\overline{A}_1\overline{A}_2 - 3A_3|A_3|^2 - 6A_3(|A_1|^2 + |A_2|^2) &= 0\end{aligned}\quad (3.14)$$

with  $A_j(\zeta) = A_j(X - \tilde{c}T)$  and

$$\zeta = X - \tilde{c}T = \varepsilon(x_1 - ct) = \varepsilon\xi. \quad (3.15)$$

We emphasize that it seems impossible to prove the existence of modulated fronts directly by using only the Ginzburg–Landau equation (3.14). The reason is that the approximation of the Swift–Hohenberg equation by the Ginzburg–Landau system (3.13) is only valid over large but finite intervals in the spatial travelling-wave coordinate  $\zeta$  (see Appendix A).

### 3.6 Taylor expansion of the reduced vector field

Our goal is to relate the reduced vector field

$$\frac{d}{d\xi} \mathcal{V}^c = \mathcal{M}\mathcal{V}^c + P^c \mathcal{N}(\mathcal{V}^c + h(\mathcal{V}^c)), \quad (3.16)$$

to the travelling-wave ODE (3.14) of the Ginzburg–Landau system (3.13). The idea is to show that solutions on the center manifold coincide with (3.12), up to order  $O(\varepsilon^2)$ , in the scaling suggested by (3.15). As a result, these solutions satisfy the ODE (3.14).

Recall that  $\mathcal{V}^c$  is contained in the ball of radius  $\varepsilon^{\frac{3}{4}+\gamma}$  centered at the origin in the center space  $E^c$  of the operator  $\mathcal{M}$ . It is more convenient to use the variable  $\mathcal{V}_0^c$  in the twelve-dimensional generalized null space  $E_0^c$  of  $\mathcal{M}_0$ , where the subscript 0 refers to evaluation at  $\varepsilon = 0$ . The map  $\mathcal{V}_0^c \mapsto \mathcal{V}^c := P^c \mathcal{V}_0^c$  is an isomorphism and gives the coordinate  $\mathcal{V}^c$ . We collect various estimates that we shall need below:

$$h(\mathcal{V}^c) = O(|\mathcal{V}^c|^2), \quad \mathcal{N}(\mathcal{V}) = O(\varepsilon|\mathcal{V}|^2 + |\mathcal{V}|^3), \quad P^c - P_0^c = O(\varepsilon). \quad (3.17)$$

Note that the last estimate is a consequence of the block-diagonal form of the operator  $\mathcal{M}$  in Fourier space. The analysis in § 3.5 suggests to seek solutions of order  $\varepsilon$ . Thus, if we restrict to  $\mathcal{V}_0^c = O(\varepsilon)$ , we have

$$\mathcal{V}^c = \mathcal{V}_0^c + O(\varepsilon^2), \quad h(\mathcal{V}^c) = O(\varepsilon^2), \quad \mathcal{N}(\mathcal{V}^c + h(\mathcal{V}^c)) = \mathcal{N}(\mathcal{V}_0^c) + O(\varepsilon^4).$$

Substitution of  $\mathcal{V}^c = P^c \mathcal{V}_0^c$  and the above estimates into (3.16) leads to

$$P^c \frac{d\mathcal{V}_0^c}{d\xi} = P^c [\mathcal{M}\mathcal{V}_0^c + \mathcal{N}(\mathcal{V}_0^c) + O(\varepsilon^4)] \quad (3.18)$$

which is valid for  $\mathcal{V}_0^c = O(\varepsilon)$ .

So far, we have used only abstract theory but not any specific information about the underlying PDE. In the next step, we exploit the structure of the operator  $\mathcal{M}$ . We denote by  $\mathcal{M}_0$  the operator  $\mathcal{M}$  for  $\varepsilon = 0$ . In § 3.3, we established that  $\mathcal{M}_0$ , restricted to the twelve-dimensional generalized eigenspace  $E_0^c$  associated with the eigenvalue  $v = 0$ , consists of six Jordan-blocks of length two. The six eigenvectors  $\phi_j$  of the relevant matrix  $\mathcal{M}_{\ell_1, \ell_2}$  for  $\varepsilon = 0$  are given by

$$\phi_j = \left( 1, i \left( \ell_1 + \frac{i\ell_2}{2} \right), \left[ i \left( \ell_1 + \frac{i\ell_2}{2} \right) \right]^2, \left[ i \left( \ell_1 + \frac{i\ell_2}{2} \right) \right]^3 \right) \quad (3.19)$$

for  $j = 1, 2, 3$  plus the complex conjugates. The associated generalized eigenvectors are denoted by  $\phi_j^*$ . We remark that

$$\mathcal{M}_{\ell_1, \ell_2} \phi_j = O(\varepsilon^2) \quad (3.20)$$

for  $\varepsilon \neq 0$  which can be seen by applying  $\mathcal{M}_{\ell_1, \ell_2}$  in (3.6) to the corresponding vector  $\phi_j$  in (3.19). Any element  $\mathcal{V}_0^c \in E_0^c$  is then of the form

$$\begin{aligned} \mathcal{V}_0^c &= \mathcal{Z}_1 \phi_1 e^{ip_1} + \mathcal{Z}_2 \phi_2 e^{i(-\frac{1}{2}p_1 + \frac{\sqrt{3}}{2}p_2)} + \mathcal{Z}_3 \phi_3 e^{i(-\frac{1}{2}p_1 - \frac{\sqrt{3}}{2}p_2)} + \text{c.c.} \\ &\quad + \mathcal{Z}_1^* \phi_1^* e^{ip_1} + \mathcal{Z}_2^* \phi_2^* e^{i(-\frac{1}{2}p_1 + \frac{\sqrt{3}}{2}p_2)} + \mathcal{Z}_3^* \phi_3^* e^{-i(\frac{1}{2}p_1 + \frac{\sqrt{3}}{2}p_2)} + \text{c.c.} \end{aligned} \quad (3.21)$$

where  $\mathcal{Z} = (\mathcal{Z}_1, \mathcal{Z}_2, \mathcal{Z}_3) \in \mathbb{C}^3$  and  $\mathcal{Z}^* = (\mathcal{Z}_1^*, \mathcal{Z}_2^*, \mathcal{Z}_3^*) \in \mathbb{C}^3$  are complex-valued amplitudes. To simplify notation, we use the shortcut

$$\mathcal{V}_0^c = Z \Phi_0 + Z^* \Phi_0^*$$

for (3.21). Due to the results in the last section, see in particular (3.15), we are interested

in  $\mathcal{V}_0^c = O(\varepsilon)$  and the scaled evolution variable  $\zeta = \varepsilon\xi$ . Thus, we consider the scaling

$$Z(\xi) := \varepsilon B(\varepsilon\xi) = \varepsilon B(\zeta), \quad Z^*(\xi) := \varepsilon^2 B_*(\varepsilon\xi) = \varepsilon^2 B_*(\zeta), \quad (3.22)$$

so that

$$\mathcal{V}_0^c = \varepsilon B(\varepsilon\xi)\Phi_0 + \varepsilon^2 B_*(\varepsilon\xi)\Phi_0^*.$$

Substitution into (3.18) gives

$$P^c[\varepsilon^2(B'\Phi_0 + \varepsilon B'_*\Phi_0^*)] = P^c[\varepsilon\mathcal{M}(B\Phi_0 + \varepsilon B_*\Phi_0^*) + \mathcal{N}(B\Phi_0 + \varepsilon B_*\Phi_0^*) + O(\varepsilon^4)],$$

where  $\frac{d}{d\xi} = '$ . Note that  $\mathcal{M}_0\Phi_0 = O(\varepsilon^2)$  which is a consequence of (3.20). Using this fact as well as (3.17), we get

$$\begin{aligned} P^c[\varepsilon^2(B'\Phi_0 + \varepsilon B'_*\Phi_0^*)] \\ = P^c[\varepsilon B P_0^c \mathcal{M}\Phi_0 + \varepsilon^2 B_*\Phi_0 + \varepsilon^2 B_*(\Phi_0 - \mathcal{M}\Phi_0^*) + P_0^c \mathcal{N}(B\Phi_0 + \varepsilon B_*\Phi_0^*) + O(\varepsilon^4)]. \end{aligned}$$

Comparing coefficients, and using  $\mathcal{M}_0\Phi_0 = O(\varepsilon^2)$  as well as  $\Phi_0 - \mathcal{M}\Phi_0^* = O(\varepsilon)$ , we therefore conclude that

$$B' = B_* + O(\varepsilon), \quad B'_* = G(B, B_*) + O(\varepsilon)$$

that is

$$B'' = G(B, B_*) + O(\varepsilon) \quad (3.23)$$

for a unique well-defined function  $G(B, B_*)$  that does not depend upon the function  $h(\mathcal{V})$ . It remains to determine the function  $G(B, B_*)$ . Using (3.21) and the results that we obtained so far, we know that each solution on the center manifold in the spatial dynamics is given by

$$\mathcal{V}(\xi) = \varepsilon \left[ B_1(\zeta) \phi_1 e^{ip_1} + B_2(\zeta) \phi_2 e^{i(-\frac{1}{2}p_1 + \frac{\sqrt{3}}{2}p_2)} + B_3(\zeta) \phi_3 e^{i(-\frac{1}{2}p_1 - \frac{\sqrt{3}}{2}p_2)} + \text{c.c.} \right] + O(\varepsilon^2).$$

Substituting the expression for the eigenvectors  $\phi_j$ , we see that the first component of  $\mathcal{V}(\xi)$  is given by

$$\mathcal{V}_1(\xi) = \varepsilon B_1(\zeta) e^{ix_1} + \varepsilon B_2(\zeta) e^{i(-\frac{1}{2}x_1 + \frac{\sqrt{3}}{2}x_2)} + \varepsilon B_3(\zeta) e^{i(-\frac{1}{2}x_1 - \frac{\sqrt{3}}{2}x_2)} + \text{c.c.} + O(\varepsilon^2) \quad (3.24)$$

where  $\xi$  and  $\zeta$  are related via (3.15). Here, we have also used that  $(p_1, p_2) = (x_1, x_2)$ , see section 3.1. A comparison of (3.12) and (3.24) shows that they are identical up to terms of order  $\varepsilon^2$  once we take (3.15) into account. Our analysis in this section shows that the higher-order terms do not change the nonlinearity  $G$  in (3.23). Thus, (3.23) coincides necessarily with (3.14).

In summary, the amplitudes  $B_j$  appearing in (3.21) and (3.22) satisfy the second-order equation

$$\begin{aligned} 4\partial_\zeta^2 B_1 + \tilde{\epsilon}\partial_\zeta B_1 + \tilde{\mu}B_1 - \tilde{\beta}\overline{B}_2\overline{B}_3 - 3B_1|B_2|^2 - 6B_1(|B_2|^2 + |B_3|^2) + O(\varepsilon) &= 0 \\ \partial_\zeta^2 B_2 + \tilde{\epsilon}\partial_\zeta B_2 + \tilde{\mu}B_2 - \tilde{\beta}\overline{B}_3\overline{B}_1 - 3B_2|B_3|^2 - 6B_2(|B_3|^2 + |B_1|^2) + O(\varepsilon) &= 0 \\ \partial_\zeta^2 B_3 + \tilde{\epsilon}\partial_\zeta B_3 + \tilde{\mu}B_3 - \tilde{\beta}\overline{B}_1\overline{B}_2 - 3B_3|B_1|^2 - 6B_3(|B_1|^2 + |B_2|^2) + O(\varepsilon) &= 0 \end{aligned} \quad (3.25)$$

as claimed.

#### 4 Analysis of the reduced system

In this section, we seek heteroclinic orbits to (3.25) that correspond to modulated fronts of the Swift–Hohenberg equation (1.1). These heteroclinic orbits lie in the four-dimensional invariant subspace defined by  $B_1 \in \mathbb{R}$  and  $B_2 = B_3 \in \mathbb{R}$  of the ambient twelve-dimensional phase space. The invariance of the lower-dimensional subspace is enforced by reflection symmetry.

We note that the terms of order  $O(\varepsilon)$  represent a regular perturbation of (3.25) with  $\varepsilon = 0$ . The heteroclinic orbits that we find below are constructed as transverse intersections of the stable and unstable manifolds belonging to hyperbolic equilibria. We therefore set  $\varepsilon = 0$  in this section since each connection of the above type found for  $\varepsilon = 0$  persists for  $\varepsilon \neq 0$  due to transversality.

Thus, consider (3.25) restricted to  $B_1 \in \mathbb{R}$  and  $B_2 = B_3 \in \mathbb{R}$ , and with  $\varepsilon = 0$ :

$$\begin{aligned} 4\partial_\zeta^2 B_1 + \tilde{c}\partial_\zeta B_1 + \tilde{\mu}B_1 - \tilde{\beta}B_2^2 - 3B_1^3 - 12B_1B_2^2 &= 0 \\ \partial_\zeta^2 B_2 + \tilde{c}\partial_\zeta B_2 + \tilde{\mu}B_2 - \tilde{\beta}B_1B_2 - 9B_2^3 - 6B_1^2B_2 &= 0. \end{aligned} \quad (4.1)$$

We note that any solution  $(B_1, B_2)(\zeta) \in \mathbb{R}^2$  of (4.1) corresponds to a modulated wave of the Swift–Hohenberg equation of the form

$$\begin{aligned} u(x_1, x_2, t) &= v(x_1 - ct, x_1, x_2) \\ &= 2\varepsilon \left[ B_1(\varepsilon(x_1 - ct)) \cos x_1 + 2B_2(\varepsilon(x_1 - ct)) \cos \frac{x_1}{2} \cos \frac{\sqrt{3}x_2}{2} \right] + O(\varepsilon^2), \end{aligned} \quad (4.2)$$

where  $\zeta = \varepsilon(x_1 - ct) = \varepsilon\xi$ . See (3.1), (3.4) and (3.24).

Throughout the rest of this section, we assume that  $\tilde{\beta} < 0$ , so that stable hexagons are supported. We will also, for the sake of simplicity and due to the scaling properties of (4.1), omit the tildes in (4.1). Finally, we use the notation  $B = (B_1, B_2)$ .

##### 4.1 Modulated fronts with large wave speeds

We analyse (4.1) in the limit of large wave speeds  $c \gg 1$  which allows us to study (4.1) as a singular-perturbation problem. Thus, we define a new independent variable  $\rho = \zeta/c$ , so that (4.1) becomes

$$\begin{aligned} \partial_\rho B_1 &= B_1^*, & \frac{4}{c^2} \partial_\rho B_1^* &= -B_1^* - \mu B_1 + \beta B_2^2 + 3B_1^3 + 12B_1B_2^2 \\ \partial_\rho B_2 &= B_2^*, & \frac{1}{c^2} \partial_\rho B_2^* &= -B_2^* - \mu B_2 + \beta B_1B_2 + 9B_2^3 + 6B_1^2B_2 \end{aligned} \quad (4.3)$$

when written as a first-order system. The above system is the slow system in the sense of geometric singular perturbation theory [28]. The associated fast system is obtained by rescaling time according to  $\tau = c^2\rho$  which gives

$$\begin{aligned} \partial_\tau B_1 &= \frac{1}{c^2} B_1^*, & 4\partial_\tau B_1^* &= -B_1^* - \mu B_1 + \beta B_2^2 + 3B_1^3 + 12B_1B_2^2 \\ \partial_\tau B_2 &= \frac{1}{c^2} B_2^*, & \partial_\tau B_2^* &= -B_2^* - \mu B_2 + \beta B_1B_2 + 9B_2^3 + 6B_1^2B_2. \end{aligned} \quad (4.4)$$

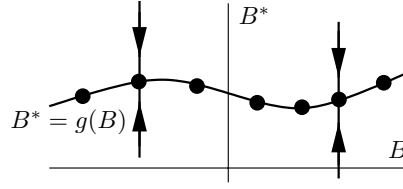


FIGURE 4. The two-dimensional normally-hyperbolic slow manifold of (4.4) for  $\varepsilon = 0$ .

Setting  $1/c^2 = 0$  in (4.4), we obtain

$$\begin{aligned}\partial_\tau B_1 &= 0, & 4\partial_\tau B_1^* &= -B_1^* - \mu B_1 + \beta B_2^2 + 3B_1^3 + 12B_1 B_2^2 \\ \partial_\tau B_2 &= 0, & \partial_\tau B_2^* &= -B_2^* - \mu B_2 + \beta B_1 B_2 + 9B_2^3 + 6B_1^2 B_2.\end{aligned}$$

This system has a two-dimensional manifold of equilibria, given by

$$(B_1^*, B_2^*) = g(B_1, B_2) = (-\mu B_1 + \beta B_2^2 + 3B_1^3 + 12B_1 B_2^2, -\mu B_2 + \beta B_1 B_2 + 9B_2^3 + 6B_1^2 B_2),$$

which is normally hyperbolic and, in fact, attracting (see Figure 4). The flow on this slow manifold, computed by using the limit  $1/c^2 = 0$  of the slow system (4.3), is given by

$$\begin{aligned}\partial_\rho B_1 &= -\mu B_1 + \beta B_2^2 + 3B_1^3 + 12B_1 B_2^2 \\ \partial_\rho B_2 &= -\mu B_2 + \beta B_1 B_2 + 9B_2^3 + 6B_1^2 B_2.\end{aligned}\tag{4.5}$$

Geometric singular perturbation theory [18, 28] shows that the slow manifold persists for  $1/c^2 \neq 0$  as an invariant manifold, and that the flow on the slow manifold is given by (4.5) up to terms of order  $O(1/c^2)$ . Thus, the terms of higher order on the slow manifold can again be viewed as regular perturbations that do not destroy transversely constructed heteroclinic orbits between hyperbolic equilibria.

Therefore, we focus on the planar vector field (4.5). First, note that (4.5) is equivariant with respect to the  $\mathbb{Z}_2$ -symmetry  $B_2 \mapsto -B_2$ . Consequently, the  $B_1$ -axis is invariant under the flow of (4.5). Note that the lines  $B_1 = \pm B_2$  are also invariant. Secondly, we remark that the function

$$\mathcal{L}(B) = \mu \left[ \frac{B_1^2}{2} + B_2^2 \right] - \beta B_1 B_2^2 - \frac{3}{4} B_1^4 - 6B_1^2 B_2^2 - \frac{9}{2} B_2^4$$

is a Lyapunov functional for (4.5) since we have  $\langle \nabla \mathcal{L}(B), F(B) \rangle = -F_1(B)^2 - 2F_2(B)^2$  where we denote by  $F(B) = (F_1(B), F_2(B))$  the right-hand side of (4.5).

We analyse the equilibria of (4.5) next. Thus, we have to solve the equation

$$-\mu B_1 + \beta B_2^2 + 3B_1^3 + 12B_1 B_2^2 = 0\tag{4.6}$$

$$(-\mu + \beta B_1 + 9B_2^3 + 6B_1^2) B_2 = 0.\tag{4.7}$$

Equation (4.7) is satisfied for  $B_2 = 0$  and for  $9B_2^2 = \mu - \beta B_1 - 6B_1^2$ . In the first case, upon substituting  $B_2 = 0$  into (4.6), we see that (4.6) has the solutions  $B = 0$  corresponding to the trivial state and  $B_{\text{rolls}} = (\pm\sqrt{\mu/3}, 0)$  corresponding to the rolls. In the second case, we

substitute the expression  $9B_2^2 = \mu - \beta B_1 - 6B_1^2$  into (4.6) to get

$$\begin{aligned} -\mu B_1 + (\beta + 12B_1)B_2^2 + 3B_1^3 &= -\mu B_1 + \frac{1}{9}(\beta + 12B_1)(\mu - \beta B_1 - 6B_1^2) + 3B_1^3 \\ &= \frac{1}{9}(3B_1 + \beta)(\mu - \beta B_1 - 15B_1^2) = 0. \end{aligned}$$

Thus, we recover the hexagons from (2.5) for  $\mu = \beta B_1 + 15B_1^2$  where in fact  $B_1 = B_2$ . We also obtain the solutions  $B_{mm} = (-\beta/3, \pm\sqrt{\mu - \beta^2/3}/3)$  which exist for  $\mu \geq \beta^2/3$ . Note that these mixed-mode solutions (which were called wavy rolls in Buzano & Golubitsky [5]) bifurcate from the rolls in a pitchfork bifurcation (breaking the  $B_2 \mapsto -B_2$  symmetry) at  $\mu = \beta^2/3$ , and cross the branch of hexagons, located on the invariant line  $B_1 = B_2$ , via a transcritical bifurcation at  $\mu = 4\beta^2/3$ , where the two components of  $B_{mm}$  coincide. We refer to Figure 2 for the bifurcation diagram.

The eigenvalue structure of the linearization of (4.5) about the various equilibria is as follows. The trivial state  $B = 0$  has a double eigenvalue at  $v = -\mu$ . The rolls have eigenvalues at  $v = 2\mu$  and at  $v = \mu + \beta\sqrt{\mu/3}$  with eigenvectors  $(1, 0)$  and  $(0, 1)$ , respectively. The hexagons have eigenvalues at  $v = \mu + 15B_1^2$  and at  $v = -2\mu + 24B_1^2$  with eigenvectors  $(1, 1)$  and  $(-2, 1)$ , respectively. Lastly, the mixed modes have one strictly positive eigenvalue, while the other eigenvalue is strictly negative for  $\mu < 4\beta^2/3$  and strictly positive for  $\mu > 4\beta^2/3$ . We omit the explicit expressions of these eigenvalues.

Finally, note that the vector field (4.5), restricted to the line segments  $\{B_1 = a, |B_2| \leq a\}$  and  $\{B_2 = a, |B_1| \leq a\}$ , points outwards for  $a \gg 1$  sufficiently large. Utilizing the resulting invariant regions and the information collected above, it is then straightforward to verify that the phase diagrams of (4.5) are as plotted in Figure 5. This also completes the bifurcation diagram in Figure 2.

Note that the evolution variable in figure 5 is the (scaled) spatial variable  $\xi$ , not time  $t$ . Each connecting orbit in figure 5 gives a modulated front of the Swift–Hohenberg equation with the spatial profile of that orbit. In particular, for  $\mu > 0$ , the temporally unstable state  $u = 0$  of the Swift–Hohenberg equation corresponds to the stable equilibrium  $B = 0$  in the spatial dynamics:  $u = 0$  can be invaded by any other equilibrium, so that connecting orbits from any other equilibrium to  $B = 0$  should exist.

Inspecting the phase diagrams shown in Figure 5, recalling that the terms of order  $O(\varepsilon)$  that we neglected constitute regular perturbations that do not change the phase diagrams, and also recalling the connection (4.2) between solutions  $(B_1, B_2)$  of (4.1) and modulated fronts  $v(\xi, x_1, x_2)$  of the Swift–Hohenberg equation, we have proved the following theorem.

**Theorem 4.1** Consider the modified Swift–Hohenberg equation (1.1) with  $\mu = \tilde{\mu}\varepsilon^2$  and  $\beta = \tilde{\beta}\varepsilon$  for some fixed  $\tilde{\beta} < 0$ , and introduce the wave speed  $c = \tilde{c}\varepsilon$ . Then there are positive numbers  $\varepsilon_0$  and  $\tilde{c}_0$  such that the following is true for every  $\varepsilon$  with  $0 < \varepsilon < \varepsilon_0$  and every  $\tilde{c}$  with  $\tilde{c} > \tilde{c}_0$ . Equation (1.1) has modulated-front solutions  $u(x_1, x_2, t) = v(x_1 - ct, x_1, x_2)$ , where  $v$  satisfies

$$v(\xi, p_1, p_2) = v\left(\xi, p_1, p_2 + \frac{4\pi}{\sqrt{3}}\right) = v\left(\xi, p_1 + 2\pi, p_2 + \frac{2\pi}{\sqrt{3}}\right),$$

that connect

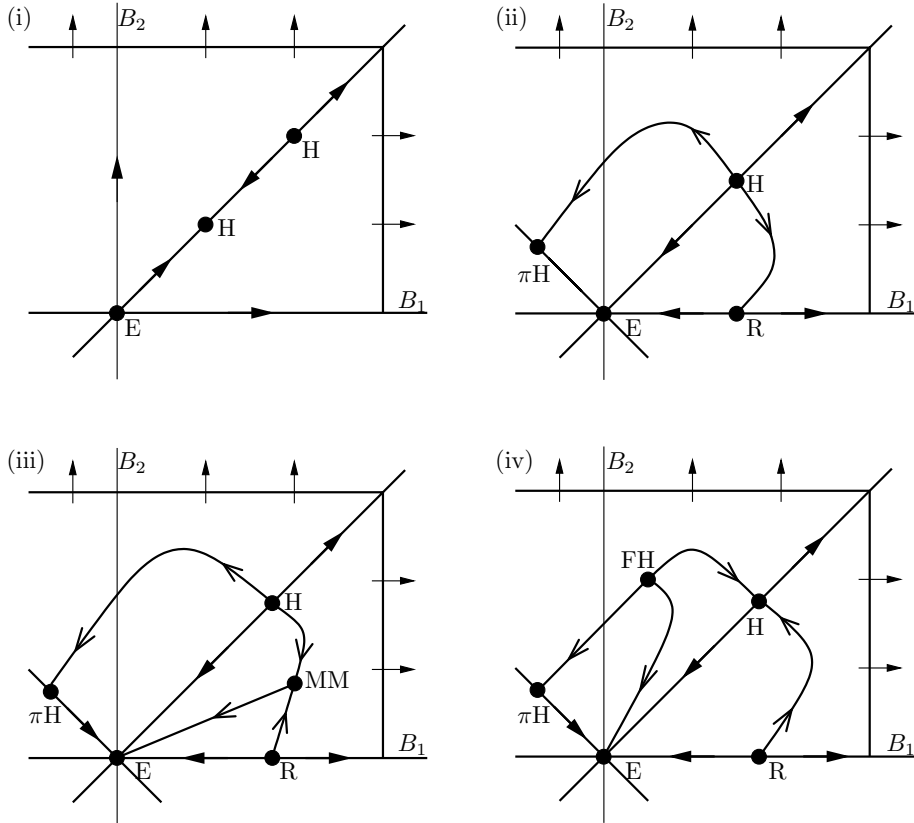


FIGURE 5. Plotted are the phase diagrams of (4.5) for fixed  $\beta < 0$ . We have  $-\beta^2/60 < \mu < 0$  in (i),  $0 < \mu < \beta^2/3$  in (ii),  $\beta^2/3 < \mu < 4\beta^2/3$  in (iii), and lastly  $4\beta^2/3 < \mu$  in (iv). The different equilibria are the trivial rest state (E), hexagons (H), rolls (R),  $\pi$ -hexagons ( $\pi H$ ), mixed modes (MM), and false hexagons (FH). Between (i) and (ii), the rolls bifurcate through a pitchfork and the  $\pi$ -hexagons through a transcritical bifurcation from  $B = 0$ . Between (ii) and (iii), the mixed modes bifurcate from the rolls in a pitchfork bifurcation. Finally, between (iii) and (iv), the mixed modes become false hexagons in a transcritical bifurcation at the hexagons. Note that there exist rolls with  $B_1 < 0$ . These rolls are unstable in the  $B_2$ -direction and connect to the  $\pi$ -hexagons for any  $\mu > 0$ . See also figure 2 for the bifurcation diagram of the Swift–Hohenberg equation.

- (i) stable hexagons  $u_{\text{hex}}$  to the unstable trivial pattern  $u = 0$  for  $0 < \mu < 4\beta^2/3$ ,
- (ii) stable hexagons  $u_{\text{hex}}$  to unstable roll solutions  $u_{\text{rolls}}$  for  $0 < \mu < \beta^2/3$ ,
- (iii) stable hexagons  $u_{\text{hex}}$  to the unstable  $\pi$ -hexagons  $u_{\pi\text{hex}}$  for  $-\beta^2/60 < \mu < 4\beta^2/3$ , and
- (iv) stable roll solutions  $u_{\text{rolls}}$  to the unstable hexagons  $u_{\text{hex}}$  for  $4\beta^2/3 < \mu$ .

In the theorem above, we say that the front  $v(\xi, p_1, p_2)$  connects the pattern  $u_{\text{left}}(p_1, p_2)$  to the pattern  $u_{\text{right}}(p_1, p_2)$  if

$$\lim_{\xi \rightarrow -\infty} \|v(\xi, \cdot, \cdot) - u_{\text{left}}(\cdot, \cdot)\|_{H^4} = 0, \quad \lim_{\xi \rightarrow \infty} \|v(\xi, \cdot, \cdot) - u_{\text{right}}(\cdot, \cdot)\|_{H^4} = 0.$$

Since we assumed that  $c > 0$ , the pattern  $u_{\text{left}}$  therefore propagates into the region occupied by  $u_{\text{right}}$ .

Besides the fronts mentioned in the above theorem, the phase diagrams in Figure 5 give the existence of additional fronts as well as the non-existence of certain fronts with large wave speed. For instance, there are fronts connecting false hexagons to hexagons but no fronts that connect rolls to  $\pi$ -hexagons.

#### 4.2 Modulating fronts connecting stable rolls to the unstable trivial pattern

Modulated fronts that connect rolls to the unstable rest state  $u = 0$  can be found for any wave speed  $c > 0$ . Indeed, consider (4.1) with  $B_2 = 0$ , which reduces to the second-order equation

$$4\partial_\zeta^2 B_1 + c\partial_\zeta B_1 + \mu B_1 - 3B_1^3 = 0. \quad (4.8)$$

The roll solutions  $B_1 = \pm\sqrt{\mu/3}$  exist for any  $\mu > 0$ . Furthermore, by inspecting the phase diagram of (4.8), heteroclinic connections between the rolls and  $B_1 = 0$  exist for any  $c > 0$ . These fronts are monotone for  $c \geq 4\sqrt{\mu}$ . They coincide, of course, with the fronts found in Collet & Eckmann [8] and Eckmann & Wayne [16] for the one-dimensional Swift–Hohenberg equation.

#### 4.3 Modulated fronts with arbitrary wave speed

Here, we comment on the existence of modulated fronts for finite, and not necessarily large, wave speeds. The relevant equation that governs the existence of such fronts is (4.1), which we rewrite as the first-order system

$$\begin{aligned} \partial_\zeta B_1 &= B_1^* \\ 4\partial_\zeta B_1^* &= -cB_1^* - \mu B_1 + \beta B_2^2 + 3B_1^3 + 12B_1 B_2^2 \\ \partial_\zeta B_2 &= B_2^* \\ \partial_\zeta B_2^* &= -cB_2^* - \mu B_2 + \beta B_1 B_2 + 9B_2^3 + 6B_1^2 B_2. \end{aligned} \quad (4.9)$$

This equation admits the Lyapunov functional

$$\mathcal{L}(B, B^*) = 2[B_1^*]^2 + [B_2^*]^2 + \mu \left[ \frac{B_1^2}{2} + B_2^2 \right] - \beta B_1 B_2^2 - \frac{3}{4} B_1^4 - 6B_1^2 B_2^2 - \frac{9}{2} B_2^4,$$

since  $\langle \nabla \mathcal{L}, F \rangle = -c([B_1^*]^2 + 2[B_2^*]^2)$ , where we denoted the right-hand side of (4.9) by  $F$ .

We note that patterns that are stable with respect to the PDE (1.1) correspond to equilibria of the spatial dynamical system (4.9) that are hyperbolic with stable and unstable manifolds each of dimension two (see Figure 6). For positive wave speeds  $c > 0$ , PDE-unstable patterns have a higher-dimensional stable manifold and a lower-dimensional unstable manifold when considered as equilibria of (4.9). In particular, the rest state  $B = 0$  has a four-dimensional stable manifold for  $\mu > 0$  and  $c > 0$ , while rolls have a three-dimensional stable manifold for  $0 < \mu < \beta^2/3$  and  $c > 0$ .

We therefore expect heteroclinic connections of saddle-saddle type, for a unique wave speed  $c$ , between PDE-stable rolls and hexagons for  $\beta^2 < 3\mu < 4\beta^2$  and between

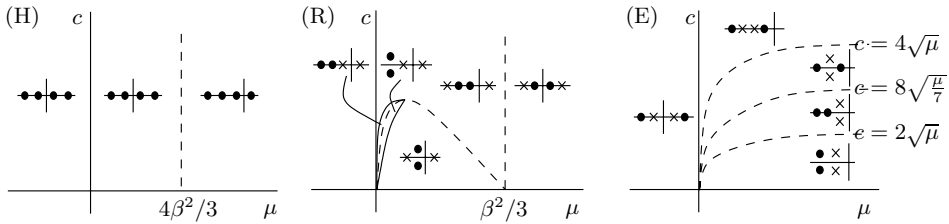


FIGURE 6. The (spatial) spectra of the linearization of (4.9) about hexagons (H), rolls (R), and the origin (E) are plotted in the parameter space  $(\mu, c)$ . For rolls and equilibria, spatial eigenvalues within the invariant subspace  $B_2 = 0$  are indicated by crosses, while the remaining two eigenvalues are plotted using bullets.

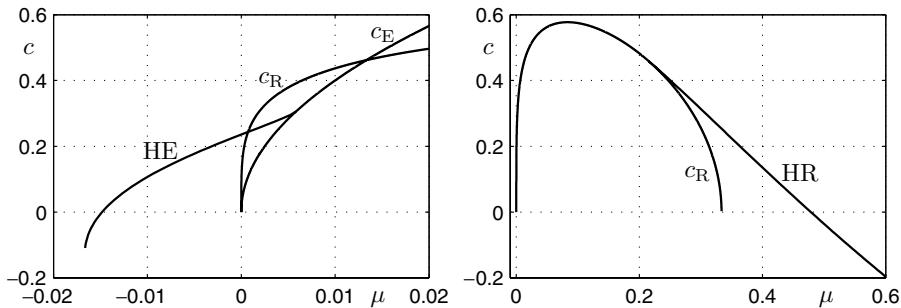


FIGURE 7. The plots show the dependence of the speed of propagation of different fronts on the parameter  $\mu$  for fixed  $\beta = -1$ . The curves labelled (HE) and (HR) are associated with stable-stable and orbit-flip fronts that connect hexagons to  $u = 0$  and hexagons to rolls, respectively. These curves were computed with AUTO97 [14]. The curves labelled  $c_E = 4\sqrt{\mu}$  and  $c_R = 2\sqrt{-\mu - \beta\sqrt{\mu/3}}$  belong to those stable-unstable fronts that are selected according to the linear marginal stability criterion. Note that  $c_E = c_R$  at  $\mu = \beta^2/75$ .

PDE-stable hexagons and the pure conductive state for  $-\beta^2 < 60\mu < 0$ . The locally unique wave speed  $c$  depends on the parameters  $\mu$  and  $\beta$ . Using HOMCONT [6] and the boundary-value solver AUTO97 [14], we have verified the existence of hexagon-rolls and hexagon-conductive fronts numerically in the parameter regime where the patterns involved are stable (see Figure 7 for the computed nonlinear dispersion relation). It appears difficult to prove the existence of connecting orbits of (4.9) analytically. Conley-index theory, as outlined in Kokubu *et al.* [31, section 3], could perhaps be used to accomplish this task. Note that the sign of the wave speed  $c$  can be calculated from the Lyapunov functional  $\mathcal{L}$ .

Of particular interest are pinned interfaces, i.e. fronts with vanishing wave speed  $c = 0$ , that correspond to spatially co-existing patterns. The curves in parameter space for which pinned fronts exist can be predicted by utilizing again the Lyapunov functional. Evaluating this functional at hexagons, rolls and the trivial rest state, and comparing the resulting energies gives the following predictions for stationary hexagon-conduction ( $\mu_{h \rightarrow 0}$ ) and

stationary hexagon-roll ( $\mu_{h \leftrightarrow r}$ ) fronts:

$$\mu_{h \leftrightarrow 0} = -\frac{2\beta^2}{135}, \quad \mu_{h \leftrightarrow r} = \frac{\beta^2(7 + 3\sqrt{6})}{30}.$$

Note that (4.9) with  $c = 0$  is reversible and Hamiltonian with energy  $\mathcal{L}$ . We remark that, even though the reduction procedure to a twelve-dimensional center manifold outlined in §2 fails for  $c = 0$ , standing interfaces can be found directly by a reduction of (1.1) with  $\partial_t u = 0$  to a spatial center manifold. The resulting reduced equations recover the above twelve-dimensional ODE with  $c = 0$ .

We note that we expect the saddle-saddle connection between PDE-stable hexagons and the stable conductive state to persist into the region where the conductive state has lost PDE-stability: in the travelling-wave ODE, the saddle-saddle connections persist as orbit-flip connections between the two-dimensional unstable manifold of the fixed point corresponding to the hexagons and the two-dimensional strong stable manifold of the origin (these fronts are also often referred to as non-generic or strongly heteroclinic fronts). Each such front is singled out as the front with steepest decay, although it is not the slowest front. We expect that this front is selected when a hexagonal pattern spreads into a region occupied by the pure conductive state (see §5 for a more detailed explanation). In particular, in this regime, the speed of propagation is not given by the minimal speed that is predicted by the linear dispersion relation (see §3.2). We refer to Figure 7 for numerical evidence of the existence of the fronts with steepest decay.

## 5 Stability of modulated fronts

We briefly outline and discuss the conjectured stability properties of the modulated fronts that we discussed above. We concentrate on stability with respect to the amplitude equation (3.13) for real  $A_1, A_2 = A_3$ , i.e. with respect to the reaction-diffusion system

$$\begin{aligned} \partial_T A_1 &= 4\partial_X^2 A_1 + \mu A_1 - \beta A_2^2 - 3A_1^3 - 12A_1 A_2^2 \\ \partial_T A_2 &= \partial_X^2 A_2 + \mu A_2 - \beta A_1 A_2 - 9A_2^3 - 6A_1^2 A_2. \end{aligned}$$

Using spatial dynamics, it is often possible to lift stability properties for Ginzburg–Landau equations back to the underlying PDE: we refer to Bridges & Mielke [3] and Mielke [33] for stability of rolls and to Schneider [43] for stability of modulating fronts (see also Sandstede & Scheel [37, 38]).

We focus on the region  $0 < \mu < \beta^2/3$  where fronts connect stable hexagons with unstable rolls and the trivial rest state. The ‘linear marginal stability’ criterion states that an interface between a stable and an unstable pattern selects the wave speed at which the unstable state is marginally stable, i.e. at the transition between convective and absolute instability. As outlined in §3.2, the resulting wave speed can be computed from the spatial eigenvalues at the unstable state. Evaluating this criterion, we see that the selected wave speeds  $c_E$  and  $c_R$  are

$$c_E = 4\sqrt{\mu}, \quad c_R = 2\sqrt{-\mu - \beta\sqrt{\frac{\mu}{3}}}$$

for fronts invading  $u = 0$  and rolls, respectively. Fronts invading rolls or the trivial state with wave speeds larger than  $c_E$  or  $c_R$ , respectively, are stable in function spaces with exponential weights. We refer elsewhere [46, 11, 15, 47] for results and references regarding the front-selection problem.

As mentioned above, however, the linear marginal stability criterion fails for those values of  $\mu$  for which orbit-flip connections are present. Indeed, in a function space with an appropriate exponential weight, these fronts have  $\lambda = 0$  as a temporal eigenvalue since they decay sufficiently fast towards their rest states. For any other stable-unstable front  $v$ ,  $\lambda = 0$  is not a temporal eigenvalue, since they decay slower, and their spatial derivative  $v'$  does therefore not lie in the exponentially-weighted function space. As a result, at the orbit-flip front with speed  $c_{\text{of}}$ , an eigenvalue crosses through the imaginary axis and destabilizes fronts with either larger or smaller wave speed than  $c_{\text{of}}$ . In fact, it is the slower fronts that typically destabilize. We again refer elsewhere [46, 11, 15, 47] for references.

Finally, we note that there is a one-parameter family of fronts, not counting the translation parameter, that connect hexagons to  $u=0$  for each fixed  $c$  in the region  $0 < 3\mu < \beta^2$ . While the eventual wave speed  $c$  of a propagating interface is selected according to either  $c = c_{\text{of}}$  or the linear marginal stability criterion, it is not clear which front among the one-parameter family belonging to the selected wave speed is chosen. We refer to Pisman & Nepomnyashchy [36], Csahók & Misbah [12] and Haragus & Nepomnyashchy [22] for interesting numerical simulations and conjectures.

## 6 Discussion

The approach outlined in this paper is well suited for planar modulated fronts where the interface between the two asymptotic patterns is approximately a straight line. In a number of experiments and numerical simulations, fronts with a radial spatial structure have also been observed. Localized and pinned, i.e. stationary, droplets of hexagons surrounded by the homogeneous rest state have been observed experimentally, for instance in the CIMA reaction [35] and in Rayleigh–Bénard convection [1], and numerically [25, Figure 9(c)] in the equation

$$\partial_t u = -(1 + \Delta)^2 u + \mu u + \gamma u^2 - u^3,$$

another variant of the Swift–Hohenberg equation. Such hexagon droplets can also propagate radially. Numerical computations of the Lengyel–Epstein model, a two-component reaction-diffusion system, reveal a droplet, formed by a large number of stable subcritical hexagons, that expands radially into the stable background state [27, Figure 10]. Experimentally in the Rayleigh–Bénard convection [1, Figure 22] and numerically in the Brusselator model [27, Figure 12], droplets formed by a large number of stable supercritical hexagons have been observed that expand into the unstable homogeneous rest state. In this case, the expanding droplet is shaped like a large hexagon (comprised of many small hexagons), and rolls appear as intermediate patterns between the hexagon droplet and the rest state. The rolls align along the edges of the hexagon droplet. We refer to De Wit [13] for more details and references. Localized, pinned structures in one spatial dimension can be explained using symmetry arguments (see, for instance, Coullet *et al.* [10]). In higher space dimensions, it is not clear how to explain the appearance

of the aforementioned localized or radially expanding hexagon droplets rigorously. The approach used in this paper certainly fails.

## Appendix A The Ginzburg–Landau system

The Ginzburg–Landau formalism can be considered as a generalization of the center-manifold theorem [42]. The properties of Ginzburg–Landau equations that are needed to make this statement more precise are attractivity [17, 40] and validity of the approximation [9, 23, 39, 44].

In this appendix, we state these results in the context of the Ginzburg–Landau system (3.13). The attractivity result shows that solutions evaluated at times of order  $O(1/\varepsilon^2)$  are spatial modulations of the most unstable Fourier modes. In detail:

**Theorem A.1** ([17, 40]) *For every  $C_1 > 0$ , there exist positive constants  $C_2$ ,  $\varepsilon_0$  and  $T_0$  such that the following is true for every  $\varepsilon \in (0, \varepsilon_0)$ . Let  $u = u(t)$  be a solution of (1.1) with  $\|u|_{t=0}\|_{C_{bdd}^4} \leq C_1 \varepsilon$ . At time  $t = T_0/\varepsilon^2$ , this solution can then be written as*

$$\begin{aligned} u(x, T_0/\varepsilon^2) \\ = \varepsilon A_1(\varepsilon x_1) e^{ix_1} + \varepsilon A_2(\varepsilon x_1) e^{i(-\frac{1}{2}x_1 + \frac{\sqrt{3}}{2}x_2)} + \varepsilon A_3(\varepsilon x_1) e^{i(-\frac{1}{2}x_1 - \frac{\sqrt{3}}{2}x_2)} + \text{c.c.} + \varepsilon^2 R(x, T_0/\varepsilon^2) \end{aligned}$$

where  $\|A_1\|_{C_{bdd}^4} + \|A_2\|_{C_{bdd}^4} + \|A_3\|_{C_{bdd}^4} + \|R\|_{C_{bdd}^4} \leq C_2$ .

Hence, the set of modulated solutions is an attractive set analogous to the center manifold in the case of discrete spectrum. The dynamics on the attractive set is approximated by the coupled Ginzburg–Landau system (3.13). In detail:

**Theorem A.2** *Let  $(A, \bar{A}) \in C([0, T_0], C_{bdd}^4)$  with  $A = (A_1, A_2, A_3)$  and  $\bar{A} = (\bar{A}_1, \bar{A}_2, \bar{A}_3)$  be a solution of the Ginzburg–Landau system (3.13), and denote by  $\psi$  the approximation defined in (3.12). Under these assumptions, there exist positive constants  $C_0$  and  $\varepsilon_0$  such that for every  $\varepsilon \in (0, \varepsilon_0)$  there is a solution  $u \in C([0, T_0], C_{bdd}^4)$  of the Swift–Hohenberg equation (1.1) that satisfies*

$$\sup_{t \in [0, T_0/\varepsilon^2]} \|u(t) - \psi(t)\|_{C_{bdd}^4} \leq C_0 \varepsilon^2.$$

**Proof** The proof given in Kirrmann *et al.* [30] applies, since we assumed that the coefficient in front of the quadratic term is of order  $O(\varepsilon)$ .  $\square$

Thus, the error of the approximation, which by the above theorem is of order  $O(\varepsilon^2)$ , is much smaller than the magnitude  $O(\varepsilon)$  of the solution  $u$  and the approximation  $\psi$ .

The above two theorems allow us to consider the approach via Ginzburg–Landau equations in systems with continuous spectrum as a generalization of the center-manifold theorem. In particular, global existence results transfer from the amplitude equations to the original system [42], and upper-semicontinuity of attractors holds [34].

### Acknowledgements

This work was supported by the Volkswagenstiftung through the *Research in Pairs* (RiP) program at the Mathematisches Forschungsinstitut Oberwolfach. B. Sandstede was also supported by the NSF under grant DMS-9971703 and by an Alfred P. Sloan Research Fellowship.

### References

- [1] BODENSCHATZ, E., PESCH, W. & AHLERS, G. (2000) Recent developments in Rayleigh–Bénard convection. *Annu. Rev. Fluid Mech.* **32**, 709–778.
- [2] BOISSONADE, J., DULOS, E. & DE KEPPEL, P. (1995) Turing patterns: from myth to reality. In: R. Kapral and K. Showalter (eds.), *Chemical Waves and Patterns*, pp. 221–268. Kluwer.
- [3] BRIDGES, T. & MIELKE, A. (1995) A proof of the Benjamin–Feir instability. *Arch. Rat. Mech. Anal.* **113**, 145–198.
- [4] BUSSE, F. H. & MÜLLER, S. C. (EDS.) (1998) *Evolution of Spontaneous Structures in Dissipative Continuous Systems: Lecture Notes in Physics*, **55**. Springer-Verlag.
- [5] BUZANO, E. & GOLUBITSKY, M. (1983) Bifurcation on the hexagonal lattice and the planar Bénard problem. *Philos. Trans. Roy. Soc. London A*, **308**, 617–667.
- [6] CHAMPNEYS, A. R., KUZNETSOV, YU. A. & SANDSTEDE, B. (1996) A numerical toolbox for homoclinic bifurcation analysis. *Int. J. Bifurcation Chaos*, **6**, 867–887.
- [7] CHOW, S.-N. & HALE, J. (1982) *Methods of bifurcation theory: Grundlehren der Mathematischen Wissenschaften*, **251**. Springer-Verlag.
- [8] COLLET, P. & ECKMANN, J.-P. (1986) The existence of dendritic fronts. *Comm. Math. Phys.* **107**, 39–92.
- [9] COLLET, P. & ECKMANN, J.-P. (1990) The time dependent amplitude equation for the Swift–Hohenberg problem. *Comm. Math. Phys.* **132**, 139–153.
- [10] COULLET, P., RIERA, C. & TRESSER, C. (2000) Stable static localized structures in one dimension. *Phys. Rev. Lett.* **84**, 3069–3072.
- [11] CROSS, M. C. & HOHENBERG, P. C. (1993) Pattern formation outside of equilibrium. *Rev. Mod. Phys.* **65**, 851–1090.
- [12] CSAHÓK, Z. & MISBAH, C. (1999) On the invasion of an unstable structureless state by a stable hexagonal pattern. *Europhys. Lett.* **47**, 331–337.
- [13] DE WIT, A. (1999) Spatial patterns and spatiotemporal dynamics in chemical systems. *Adv. Chem. Phys.* **109**, 435–511.
- [14] DOEDEL, E., CHAMPNEYS, A. R., FAIRGRIVE, T. F., KUZNETSOV, YU. A., SANDSTEDE, B. & WANG, X. (1997) AUTO97: *Continuation and bifurcation software for ordinary differential equations (with HOMCONT)*. Technical Report, Concordia University.
- [15] EBERT, U. & VAN SAARLOOS, W. (2000) Front propagation into unstable states: universal algebraic convergence towards uniformly translating pulled fronts. *Physica D* **146**, 1–99.
- [16] ECKMANN, J.-P. & WAYNE, C. E. (1991) Propagating fronts and the center manifold theorem. *Comm. Math. Phys.* **136**, 285–307.
- [17] ECKHAUS, W. (1993) The Ginzburg–Landau equation is an attractor. *J. Nonlinear Sci.* **3**, 329–348.
- [18] FENICHEL, N. (1979) Geometric singular perturbation theory for ordinary differential equations. *J. Diff. Eqn.* **31**, 53–98.
- [19] GOLUBITSKY, M., STEWART, I. & SCHAEFFER, D. G. (1988) *Singularities and groups in bifurcation theory II*. Applied Mathematical Sciences **69**, Springer-Verlag.
- [20] GUNARATNE, G. H., OUYANG, Q. & SWINNEY, H. L. (1994) Pattern formation in the presence of symmetries. *Phys. Rev. E*, **50**, 2802–2820.
- [21] HARAGUS, M. & SCHNEIDER, G. (1999) Bifurcating fronts for the Taylor–Couette problem in infinite cylinders. *Z. Angew. Math. Phys.* **50**, 120–151.

- [22] HARAGUS, M. & NEPOMNYASHCHY, A. A. (2000) Nonpotential effects in dynamics of fronts between convection patterns. *Phys. Rev. E*, **61**, 4835–4847.
- [23] VAN HARTEN, R. (1991) On the validity of Ginzburg–Landau’s equation. *J. Nonlinear Sci.* **1**, 397–422.
- [24] HENRY, D. (1981) *Geometric Theory of Semilinear Parabolic Equations. Lecture Notes in Mathematics*, **840**. Springer-Verlag.
- [25] HILALI, M. F., METENS, S., BORCKMANS, P. & DEWEL, G. (1995) Pattern selection in the generalized Swift–Hohenberg model. *Phys. Rev. E*, **51**, 2046–2052.
- [26] IOOSS, G. & MIELKE, A. (1991) Bifurcating time-periodic solutions of Navier–Stokes equations in infinite cylinders. *J. Nonlinear Sci.* **1**, 107–146.
- [27] JENSEN, O., PENNBACKER, V. O., MOSEKILDE, E., DEWEL, G. & BORCKMANS, P. (1994) Localized structures and front propagation in the Lengyel–Epstein model. *Phys. Rev. E*, **50**, 736–749.
- [28] JONES, C. K. R. T. (1995) Geometric singular perturbation theory. In: *Dynamical Systems: Lecture Notes in Mathematics*, **1609**, pp. 44–118 Springer-Verlag.
- [29] KIRCHGÄSSNER, K. (1982) Wave solutions of reversible systems and applications. *J. Diff. Eqns.* **45**, 113–127.
- [30] KIRRMAN, K., SCHNEIDER, G. & MIELKE, A. (1992) The validity of modulation equations for extended systems with cubic nonlinearities. *Proc. Roy. Soc. Edinburgh*, **122A**, 85–91.
- [31] KOKUBU, H., MISCHAIKOW, K. & OKA, H. (1999) Directional transition matrix. *Conley Index Theory*, Banach Center Publ. **47**, 133–144.
- [32] LIN, G., GAO, H., DUAN, J. & ERVIN, V. (2000) Asymptotic dynamical difference between the nonlocal and local Swift–Hohenberg models. *J. Math. Phys.* **41**, 2077–2089.
- [33] MIELKE, A. (1997) Instability and stability of rolls in the Swift–Hohenberg equation. *Comm. Math. Phys.* **189**, 829–853.
- [34] MIELKE, A. & SCHNEIDER, G. (1995) Attractors for modulation equations on unbounded domains—existence and comparison. *Nonlinearity*, **8**, 743–768.
- [35] OUYANG, Q. & SWINNEY, H. L. (1995) Onset and beyond Turing pattern formation. In: Kapral, R. and Showalter, K. (eds.), *Chemical Waves and Patterns*, pp. 269–295. Kluwer.
- [36] PISMEN, L. M. & NEPOMNYASHCHY, A. A. (1994) Propagation of the hexagonal pattern. *Europhys. Lett.* **27**, 433–436.
- [37] SANDSTEDE, B. & SCHEEL, A. (2001) Essential instabilities of fronts: bifurcation, and bifurcation failure. *Dynamical Systems*, **16**, 1–28.
- [38] SANDSTEDE, B. & SCHEEL, A. (2001) On the structure of spectra of modulated travelling waves. *Math. Nachr.* **232**, 39–93.
- [39] SCHNEIDER, G. (1994) Error estimates for the Ginzburg–Landau approximation. *Z. Angew. Math. Phys.* **45**, 433–457.
- [40] SCHNEIDER, G. (1995) Analyticity of Ginzburg–Landau modes. *J. Diff. Eqns.* **121**, 233–257.
- [41] SCHNEIDER, G. (1995) Justification of modulation equations in domains with  $n \geq 2$  unbounded space directions. In: Mielke, A. & Kirchgässner, K. (eds.), *Structure and Dynamics of Nonlinear Waves in Fluids*, pp. 383–391. World Scientific.
- [42] SCHNEIDER, G. (1999) Global existence results for pattern forming processes in infinite cylindrical domains — Applications to 3D Navier–Stokes problems. *J. Math. Pures Appl.* **78**, 265–312.
- [43] SCHNEIDER, G. (2000) Existence and stability of modulating pulse-solutions in a phenomenological model of nonlinear optics. *Physica D*, **140**, 283–293.
- [44] TAKÁČ, P., BOLLERMAN, P., DOELMAN, A., VAN HARTEN, A. & TITI, E. S. (1996) Analyticity of essentially bounded solutions to semilinear parabolic systems and validity of the Ginzburg–Landau equation. *SIAM J. Math. Anal.* **27**, 424–448.
- [45] VANDERBAUWHEDE, A. & IOOSS, G. (1992) Centre manifold theory in infinite dimensions. *Dynamics Reported*, **1**, 125–163.
- [46] VAN SAARLOOS, W. (1989) Front propagation into unstable states II: linear versus nonlinear marginal stability and rate of convergence. *Phys. Rev. A*, **39**, 6367–6390.
- [47] XIN, J. (2000) Front propagation in heterogeneous media. *SIAM Rev.* **42**, 161–230.